

NO-A190 204

SHORT WAVELENGTH LASERS BASED ON SELECTIVE AMPLIFIER
PROCESSES AND CORE-EXCIT. (U) STANFORD UNIV CA EDWARD L
BINZTON LAB OF PHYSICS S E HARRIS ET AL. OCT 86

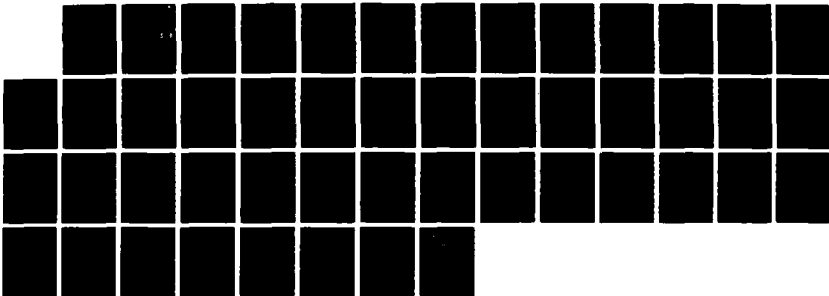
1/1

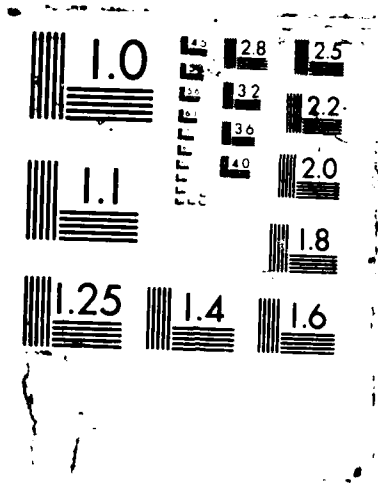
UNCLASSIFIED

NO0014-86-C-2261

F/8 9/3

ML





2nd 11/20/87

(2) ~~DTIC~~

Contract N00014-86-C-2361
Naval Research Laboratory and
Strategic Defense Initiative Organization

DTIC FILE COPY

AD-A190 204

Short Wavelength Lasers Based on
Selective Auger Processes and Core-Excited Metastable Levels

Final Technical Report for the Period
19 September 1986 — 19 March 1987

DTIC
ELECTE
JAN 14 1988
S D

Co-Principal Investigators:

S. E. Harris and J. F. Young

Edward L. Ginzton Laboratory
W. W. Hansen Laboratories of Physics
Stanford University
Stanford, CA 94305

October 1986

Contract Monitor:
Dr. Jack Davis
Code 4720
Plasma Radiation Branch
Naval Research Laboratory
4555 Overlook Ave., S.W.
Washington, DC 20375-5000

DISTRIBUTION STATEMENT A
Approved for public release
Distribution Unlimited

88 1

87

8 4 007

Section 1

Introduction

The goal of this program is to investigate, both theoretically and experimentally, new approaches to constructing XUV and soft x-ray lasers. At these short wavelengths, atomic spontaneous emission times are typically less than a nanosecond and, for levels that autoionize, are often less than a few picoseconds. It is technically very difficult to excite such levels directly to produce laser action in the way that is commonly done for visible laser levels. Practical short wavelength lasers will have a significant impact in many areas of critical national interest; applications include spectroscopy of surfaces, high resolution lithography, microscopy, and holography.

The realization of the great promise of such applications, however, depends on the properties and practicality of the lasers developed. Although there is a 20 year history of proposals for XUV and soft x-ray lasers, most approaches require very high pumping powers. We have developed systems which can produce useful gain using only moderate input energies by combining the unique properties of particular atomic states with innovative experimental techniques.

To date, we have observed gain in two species: Xe at 108.9 nm, and Zn at three lines around 133 nm. We have shown that useful gains, $\exp(3.6)$, can be achieved with input energies of less than 1 J, and we have achieved small signal gains exceeding $\exp(40)$ using less than 4 J input. In the latter case, an output energy of 20 μ J in a beam with 10 mrad divergence was measured at 108.9 nm.

Our basic approach makes use of a laser-produced plasma as a source of incoherent soft x-rays. This x-ray flashlamp photoionizes atomic core electrons producing populations in highly excited states. Our early work demonstrated that this process, combined with a new geometry with the gain species surrounding the plasma target, could produce very large

<input type="checkbox"/>
<input type="checkbox"/>
<input type="checkbox"/>
<i>per its</i>
Notes



Dist	Special
<i>A-1</i>	

excited state densities with moderate input energies. Populations in excess of 10^{15} cm^{-3} were produced using less than 0.2 J of 1064 nm energy on target.

The program during this period emphasized a particular excitation process: photoionization of a core electron followed by Auger decay to produce direct inversions. These types of systems are particularly interesting because the decay is highly selective in some cases; yields as high as 25% into particular levels are possible. Thus, significant gains can be achieved using only a few joules of laser pumping energy, rather than kilojoules. We first identified and proposed such systems in Zn, Rb, and Cs.

Gain in an Auger system was first observed at LLNL by Falcone in Xe at 108.9 nm. They measured a gain of $\exp(7.2)$ using a 55 J laser. By optimizing the operating parameters, we were able to produce gains of $\exp(3.6)$ using only 1/100 of that energy, 560 mJ. A paper describing this work has been published in *Optics Letters*, and is included as Section 2. The key to this improvement is the discovery that laser-produced plasmas can produce $\sim 75 \text{ eV}$ incoherent x-rays even at an applied power density of $5 \times 10^{10} \text{ W cm}^{-2}$. Thus a moderate energy laser can be used to create a line plasma of significant length. We have also measured gain on three lines in Zn pumped by Auger decay. The gains were comparable to Xe, as expected from theory. The yield into the upper state of Zn, however, is about 10 times greater than for Xe, and the Zn system should be capable of achieving higher efficiency under the correct conditions. The Zn work is described by a preprint included as Section 3.

Our work on Auger systems showed that useful gain can be created using as little as 1 J of energy on target, but simply applying higher energy does not lead to proportionately higher gains. The way to utilize greater energy is to pump longer lengths. As the length of the gain medium increases, however, traveling wave excitation becomes essential to utilize the length. We have developed an oblique incidence geometry which produces long, synchronously pumped lengths, and have obtained single-pass gain saturation of the Xe

laser using less than 4 J. Section 4 contains a preprint of a paper describing the details of this work.

Section 2

Low Energy Pumping of a 108.9 nm Xe Auger Laser

Low Energy Pumping of a 108.9 nm Xe Auger Laser*

Guang-Yu Yin, C. P. J. Barty, D. A. King, D. J. Walker, S. E. Harris, and J. F. Young

Edward L. Ginzton Laboratory

Stanford University

Stanford, CA 94305

Abstract

We report extensive measurements of gain in the Xe III system initially observed by Kapteyn, Lee, and Falcone. The dependence of this gain on pressure, pumping pulse length, and pump energy is presented. By optimizing these parameters we have achieved a gain of $\exp(3.2)$ using only 0.56 J of 1064 nm energy on target, representing an efficiency improvement of nearly 100. Total gains as high as $\exp(6.6)$ have been measured using higher energies. Our data indicates that effective laser-produced plasmas can be created with applied power densities as low as $5 \times 10^{10} \text{ W cm}^{-2}$.

* This work was jointly supported by the U.S. Office of Naval Research, the U.S. Air Force Office of Scientific Research, the U.S. Army Research Office, the Strategic Defense Initiative Organization, and Lawrence Livermore Laboratories.

Low Energy Pumping of a 108.9 nm Xe Auger Laser*

Guang-Yu Yin, C. P. J. Barty, D. A. King, D. J. Walker, S. E. Harris, and J. F. Young

Edward L. Ginzton Laboratory

Stanford University

Stanford, CA 94305

Kapteyn, Lee, and Falcone¹ recently reported the first observation of gain at 108.9 nm in Xe⁺⁺ pumped by incoherent x-rays from a laser-produced plasma. Total gains of exp(3.6) were measured using a natural isotopic mix of Xe. We have studied the dependence of this gain on pressure, pumping pulse length, and pump energy. By optimizing these parameters we have achieved a gain of exp(3.2) using only 0.56 J of 1064 nm energy on target. This represents an efficiency improvement of nearly 100 over Ref. 1. Using higher energies, we have measured total gains as large as exp(6.6).

The key to this optimization is the discovery that laser-produced plasmas can efficiently produce the required ~ 75 eV incoherent pumping x-rays even when the applied laser power density is only 5×10^{10} W cm⁻². Thus moderate energy lasers can be used to create a line plasma of significant length. In addition, the gain region can be located close to the target without exceeding reasonable pumping flux densities. This geometry can increase the aspect ratio and reduce the effects of amplified spontaneous emission¹ (ASE); in addition, higher pressures can be used to efficiently stop the pumping x-rays in the region of interest.

Parameters of the relevant Xe levels have been reported;² a simplified energy level diagram is shown in Fig. 1. Soft x-rays emitted by the laser-produced plasma photoionize a 4d inner shell electron of neutral Xe producing Xe⁺ 4d⁹5s²5p⁶ ²D_{3/2, 5/2} population. Rapid Auger decay produces a population inversion between the Xe⁺⁺ 5s⁰5p⁶ ¹S₀ and the

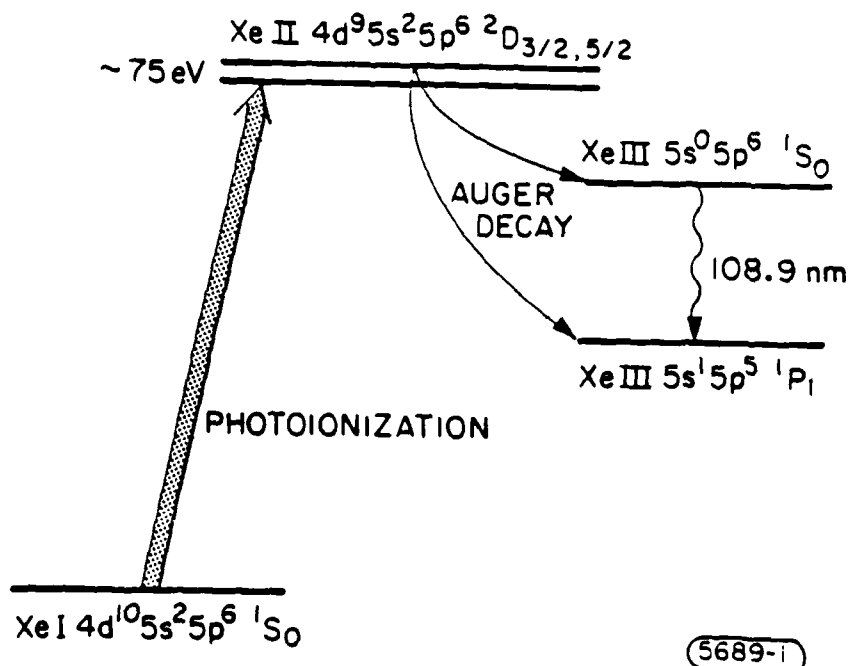
Xe⁺⁺ 5s¹5p⁵ ¹P₁ levels. The calculated Auger yield to the upper laser level is 5% and the gain cross-section is $3 \times 10^{-13} \text{ cm}^2$.

Our experimental configuration is similar to that of Ref. 1 and is shown in Fig. 2. The 1064 nm plasma-producing laser is focused by a 30 cm focal length cylindrical lens onto a solid Ta target in the Xe cell. The focal spot is a line 30 mm long by $\sim 100 \mu\text{m}$ wide, as determined by measuring the resulting target pits. A 2 mm \times 2 mm U-shaped channel and an aperture determine the pumped region observed by the detection system. The channel is positioned 2 mm from and parallel to the target, and thus, the target surface effectively forms the fourth side of the channel. The detection system consists of a 1 m normal-incidence vacuum spectrometer with a microchannel plate detector having a rise time of 350 ps. A 1 mm thick LiF window separates the Xe chamber from the spectrometer.

The length of the open side of the channel is limited to 28 mm by fixed shields in order to minimize end effects. In addition, three equal-length movable shields permit us to vary the length of the pumped region without varying the properties of the plasma pumping source. Measurements of the 108.9 nm output energy as a function of length were used to determine gain: the frequency-integrated superfluorescence output energy can be approximated as³

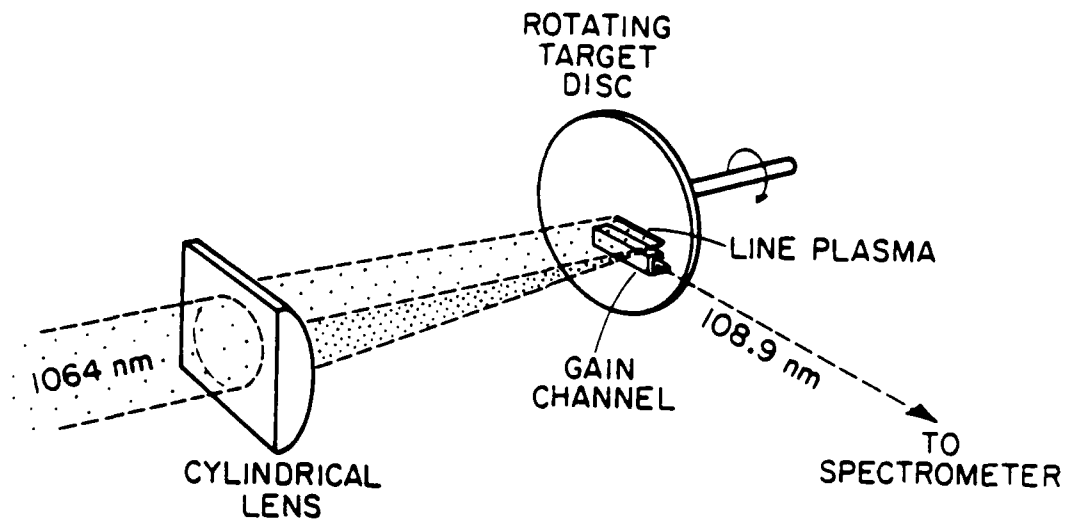
$$E \propto \frac{[\exp(\alpha l) - 1]^{3/2}}{[\alpha l \exp(\alpha l)]^{1/2}} \quad (1)$$

where α is the gain per unit length and l is length. The points in Fig. 3 are measured values of 108.9 nm energy and the curve is the best fit of Eqn. 1 to those points. In this case the fit indicates $\alpha = 2.36 \text{ cm}^{-1}$ and a total gain of $\exp(6.6)$. This curve-fitting method was used to determine all the gain values presented here. This technique, the slow time-response of the detector, and shot-to-shot variations in pumping intensity combine to limit our minimum detectable gain to $\alpha \sim 0.5 \text{ cm}^{-1}$.



5689-i

Fig. 1-Simplified energy level diagram of Xe.



5713-1

Fig. 2—Schematic of the experimental configuration. Not shown are the aperture limiting the field-of-view of the spectrometer to the volume inside the channel and the shields used to vary the active length.

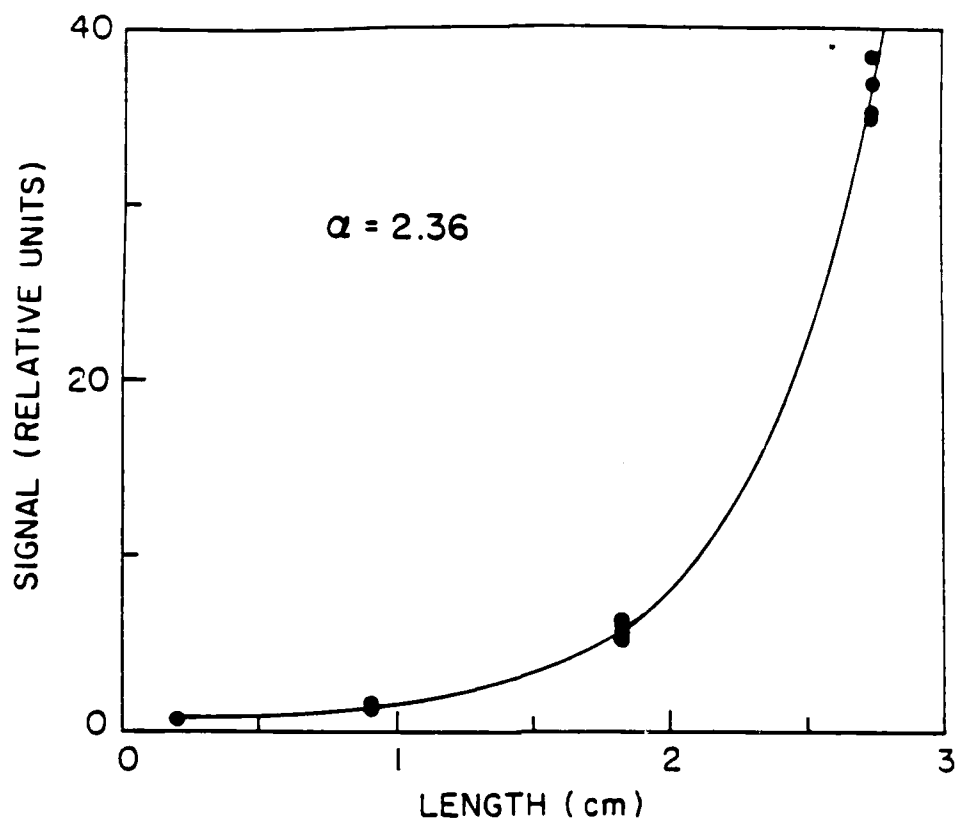
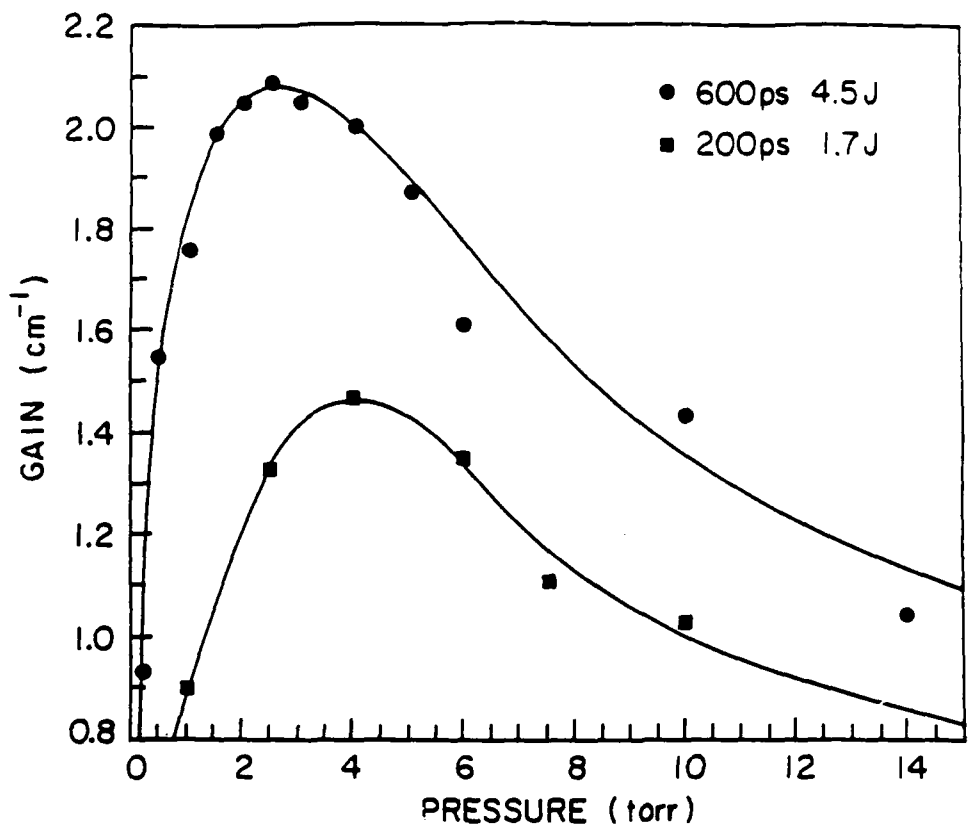


Fig. 3—Output energy at 108.9 nm as a function of pumped length for a plasma-producing laser energy of 10 J in a 600 ps pulse length, and 2.5 torr Xe pressure. The points are measured values; the curve is a plot of Eqn. 1 with $\alpha = 2.36$.

Ideally, total gain is proportional to the product of active length, pumping flux, and Xe density, but a number of processes can interact to limit the gain. We have measured the gain under a wide range of conditions in order to determine the optimum conditions. Figure 4 shows α versus pressure for two pulse lengths at constant laser power density on target. There is an optimum pressure for a given pulse length and the optimum pressure is higher for the shorter pulse. This indicates that electron quenching and/or Stark broadening may be important since raising the pressure increases not only the excited state density but also the electron density. (Reduction of the pumping flux by absorption before it reaches the active region is unimportant in our geometry.) The observed increase, however, is somewhat less than the factor of 3 expected from these effects.

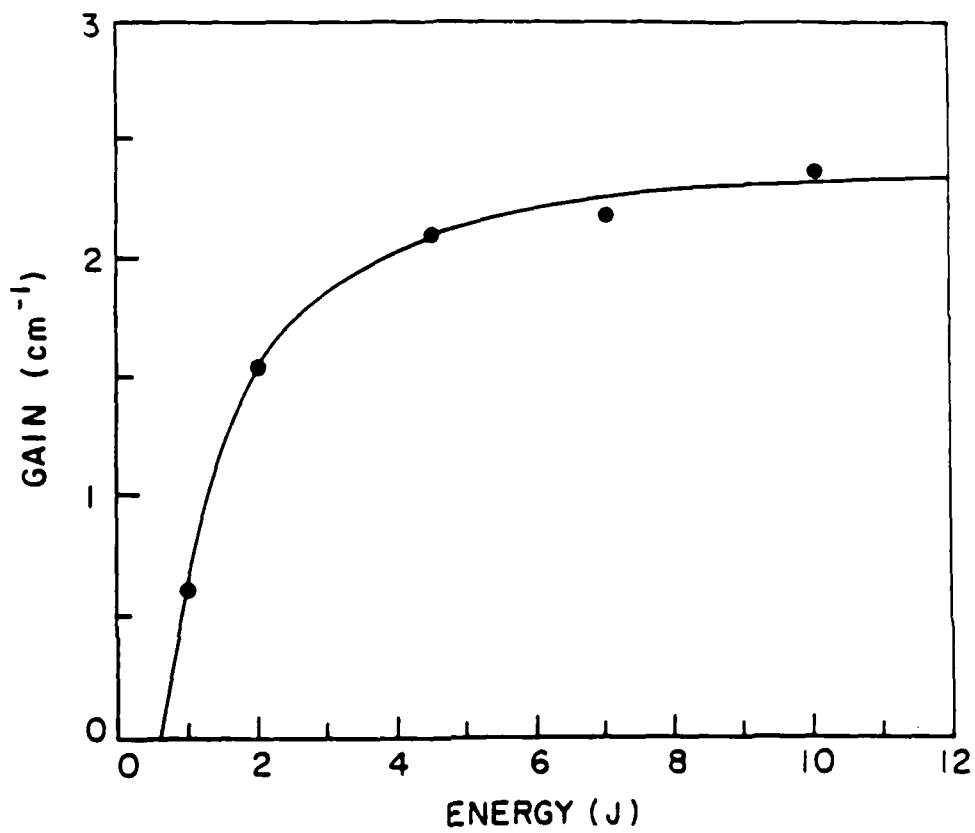
Figure 5 plots gain as a function of laser energy for a 600 ps pulse length. It is evident that some process is acting to limit the gain to $\alpha \approx 2.3$ at high energies. Faster electron quenching at the higher pumping flux densities, parasitic ASE, Stark broadening, or a combination are likely. At the other end of the scale, the gain decreases faster than linear between the 2J and 1J data points. This indicates that the laser-produced plasma at the lowest applied power density is less effective in pumping the system, either because of a lower radiating efficiency and/or a shift in spectrum. The 1064nm power density at this point is $5 \times 10^{10} \text{ W cm}^{-2}$, 20 times lower than used previously.¹ If we assume the plasma is a blackbody we can estimate its temperature from our measured gains using the parameters of the Xe system. This yields a temperature of $\sim 16 \text{ eV}$ at an applied power density of $5 \times 10^{10} \text{ W cm}^{-2}$, and a corresponding conversion efficiency of about 5% from laser to incoherent x-ray energy.

Because of the decreasing effectiveness of a plasma produced by low applied power densities, further reductions in energy can be made only by decreasing the pulse length. Figure 6 shows the gain as a function of pulse length for constant energy. At short pulse lengths the gain falls because the transit time along the channel exceeds the excitation time. For pulse lengths greater than 800 ps the gain is also reduced, probably for two



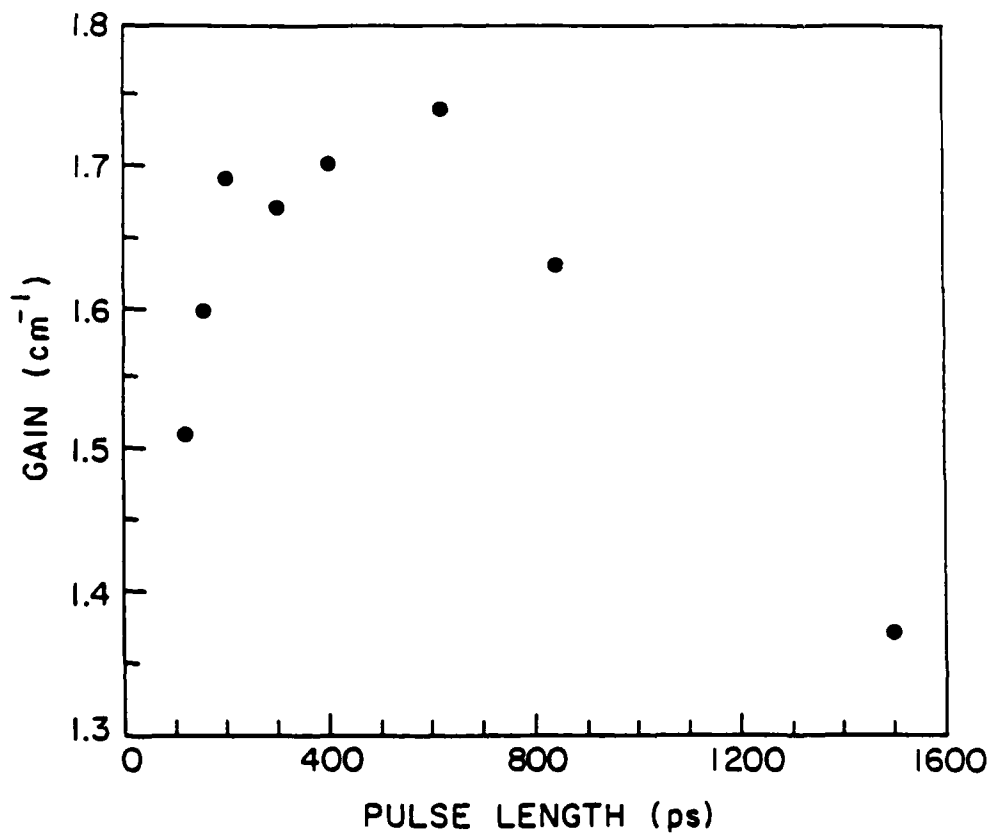
5721-2

Fig. 4—Gain coefficient as a function of pressure for excitation pulse lengths of 200 ps and 600 ps; the laser power density on target is about $1.4 \times 10^{11} \text{ W cm}^{-2}$ in both cases.



5721 -1

Fig. 5—Gain coefficient as a function of 1064 nm laser energy on target; the pulse length was 600 ps and the pressure was 2.5 torr.



5721-3

Fig. 6—Gain as a function of pulse length for a constant energy of 2.5 J and 4 torr Xe pressure.

reasons. First, the power density on target at 800 ps is $5 \times 10^{10} \text{ W cm}^{-2}$; as seen above, at this value the plasma is probably becoming less effective in pumping the system. Second, 800 ps is comparable to the effective lifetime of the upper laser level at these gains.

Gain measurements were made using isotopically enriched Xe (84% ^{136}Xe). Gain increases of only $\sim 10\%$ were observed, even under low-gain conditions where ASE limiting was not a problem.

This work is the first demonstration of the predictions of Mendelsohn and Harris⁴ and of Walker, Caro, and Harris⁵ that Auger lasers could be constructed using only several joules of laser pumping energy.

We acknowledge numerous helpful discussions with R. W. Falcone. C. P. J. Barty acknowledges the support of an ONR fellowship; Guang-Yu Yin is visiting from the Shanghai Institute of Optics and Fine Mechanics.

References

- * This work was jointly supported by the U.S. Office of Naval Research, the U.S. Air Force Office of Scientific Research, the U.S. Army Research Office, the Strategic Defense Initiative Organization, and Lawrence Livermore Laboratories.
1. H. C. Kapteyn, R. W. Lee, and R. W. Falcone, "Observation of a short-wavelength laser pumped by Auger decay," *Phys. Rev. Lett.* **57**, 2939-42 (1986).
 2. H. C. Kapteyn, M. M. Murnane, and R. W. Falcone, "Measurements on a proposed short wavelength laser system in xenon III," *Proc. SPIE Conf. on Multilayer Structures and Laboratory X-Ray Research* **688** (in press).
 3. G. J. Linford, E. R. Peressini, W. R. Sooy, and M. L. Spaeth, "Very long lasers," *App. Optics* **13**, 379-390 (1974).
 4. A. J. Mendelsohn and S. E. Harris, "Proposal for an extreme-ultraviolet selective autoionization laser in Zn III," *Opt. Lett.* **10**, 128-130 (1985).
 5. D. J. Walker, R. G. Caro, and S. E. Harris, "Proposal for an extreme-ultraviolet Auger laser at 63.8 nm in Cs III," *J. Opt. Soc. Am. B* **3**, 1515-18 (1986).

List of Figures

1. Simplified energy level diagram of Xe.
2. Schematic of the experimental configuration. Not shown are the aperture limiting the field-of-view of the spectrometer to the volume inside the channel and the shields used to vary the active length.
3. Output energy at 108.9 nm as a function of pumped length for a plasma-producing laser energy of 10 J in a 600 ps pulse length, and 2.5 torr Xe pressure. The points are measured values; the curve is a plot of Eqn. 1 with $\alpha = 2.36$.
4. Gain coefficient as a function of pressure for excitation pulse lengths of 200 ps and 600 ps; the laser power density on target is about $1.4 \times 10^{11} \text{ W cm}^{-2}$ in both cases.
5. Gain coefficient as a function of 1064 nm laser energy on target; the pulse length was 600 ps and the pressure was 2.5 torr.
6. Gain as a function of pulse length for a constant energy of 2.5 J and 4 torr Xe pressure.

Section 3

Saturation of the XeIII 109 nm Laser Using
Traveling-Wave Laser-Produced Plasma Excitation

**Saturation of the Xe III 109 nm Laser
Using Traveling-Wave Laser-Produced-Plasma Excitation***

M. H. Sher, J. J. Macklin, J. F. Young, and S. E. Harris

*Edward L. Ginzton Laboratory
Stanford University
Stanford, CA 94305*

Abstract

We describe the construction and operation of a 109 nm, photoionization-pumped, single-pass laser in Xe III. The laser is pumped by soft x-rays emitted from a laser-produced plasma in a traveling-wave geometry. Using a 3.5 J, 300 psec, 1064 nm laser pump pulse, we measure a small-signal gain coefficient of 4.4 cm^{-1} and a total small signal gain of $\exp(40)$. The laser is fully saturated and produces an output energy of $20 \mu\text{J}$ in a beam with 10 mrad divergence.

* This work was jointly supported by the U.S. Office of Naval Research, the U.S. Air Force Office of Scientific Research, the U.S. Army Research Office, the Strategic Defense Initiative Organization, and Lawrence Livermore National Laboratories.

Saturation of the Xe III 109 nm Laser
Using Traveling-Wave Laser-Produced-Plasma Excitation

M. H. Sher, J. J. Macklin, J. F. Young, and S. E. Harris

Edward L. Ginzton Laboratory

Stanford University

Stanford, CA 94305

This Letter describes the construction and operation of a single-pass, 109 nm, Xe III Auger laser.¹ The laser is pumped by soft x-rays, which are emitted from a laser-produced plasma in a traveling-wave geometry. Using only 3.5 J of 1064 nm pump energy in a 300 psec pulse, we measure a small-signal gain coefficient of 4.4 cm^{-1} and a total small-signal gain of $\exp(40)$. The 109 nm laser is fully saturated over the second half of its length and produces an output energy of $20 \mu\text{J}$ in a beam with 10 mrad divergence.

Population inversion of the 109 nm transition was proposed and demonstrated by Kapteyn *et al.*^{1,2} The inversion mechanism, outlined in the energy level diagram of Fig. 1, is inner-shell photoionization of a 4d electron, followed by Auger decay to Xe III. In this system, the Auger branching ratio is about 5% to both the upper and lower laser levels. The inversion results from the higher degeneracy of the lower level. Assuming only Doppler broadening, and ignoring hyperfine splitting, the gain cross section is $3 \times 10^{-13} \text{ cm}^2$.

Proposals for photoionization pumping of short wavelength lasers and for Auger-pumped short wavelength lasers were made by Duguay³ and by McGuire.⁴ The possibility of constructing such lasers at low pumping energies was delineated by the work of Caro *et al.*,⁵ Silfvast *et al.*,⁶ and Mendelsohn and Harris.⁷ Recently, Yin *et al.*⁸ showed that small-signal gain coefficients within a factor of two of those reported here could be produced with several joules of pump energy and, in addition, that the Xe III 109 nm gain can be

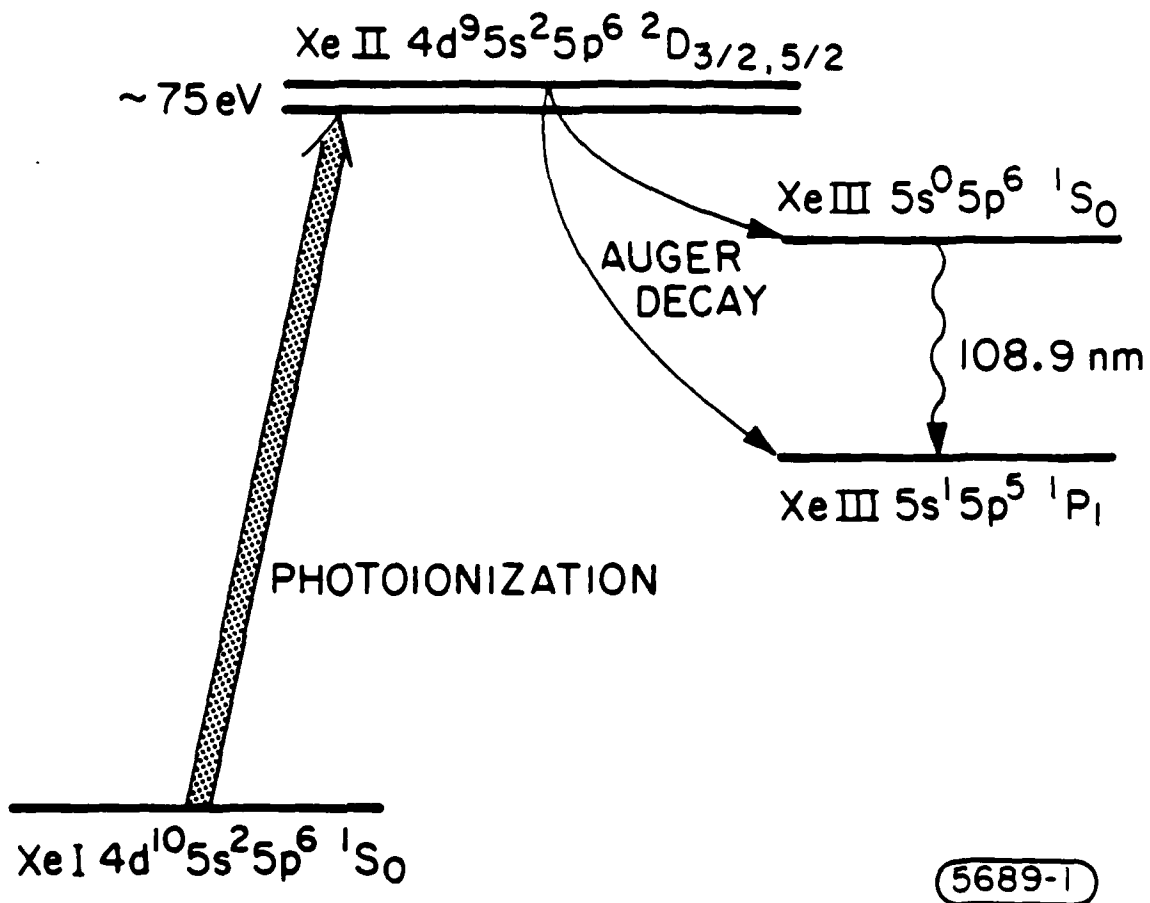


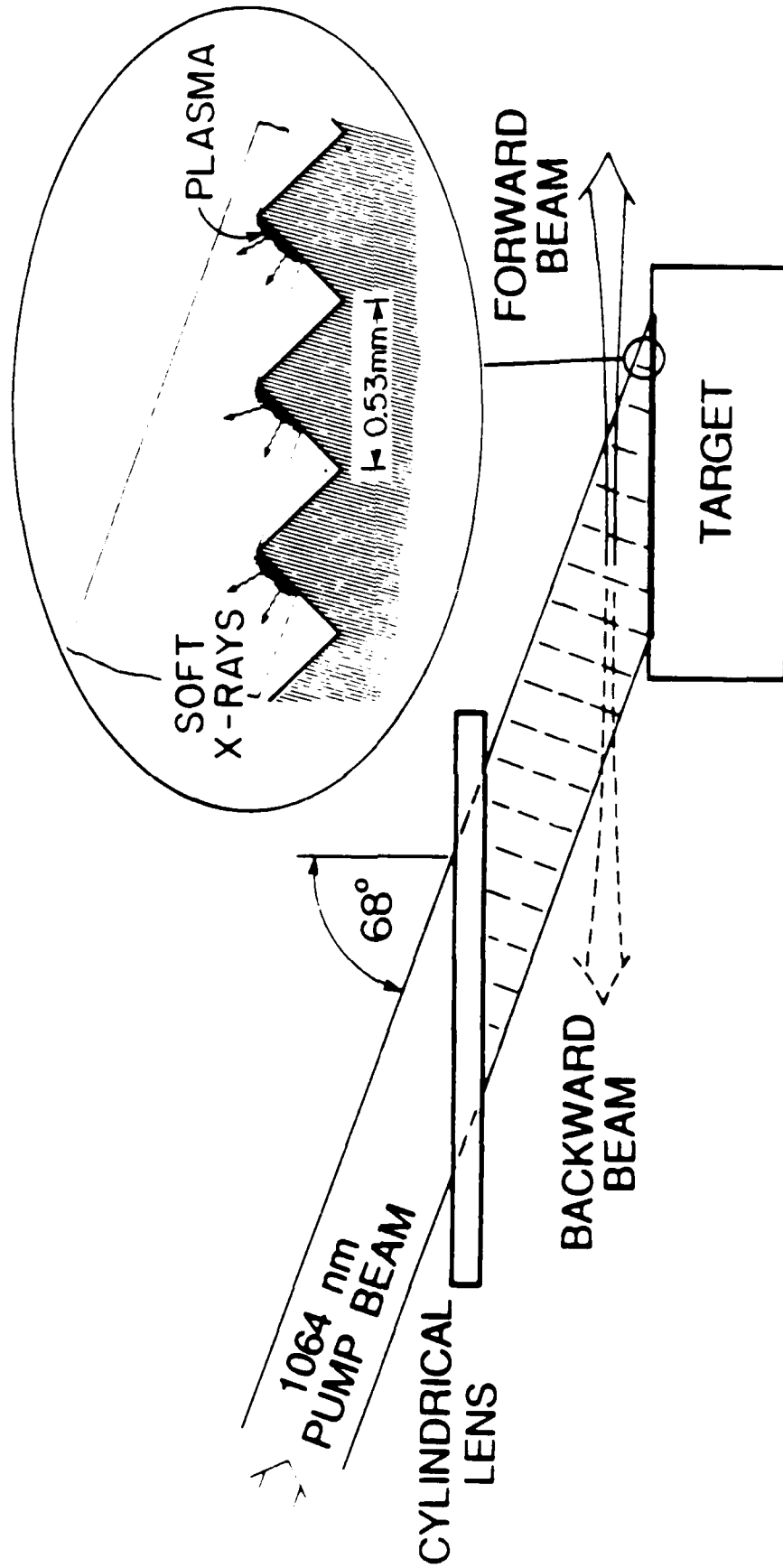
Fig. 1—Energy level diagram of Xe showing the levels relevant to photoionization and to Auger pumping of Xe III.

limited by competing processes. Their work suggests the most efficient use of pump energy requires a long, high aspect ratio geometry.

Figure 2 is a schematic diagram of the traveling-wave laser-produced-plasma excitation source. A 1064 nm laser is incident upon a cylindrical lens at $\theta = 68$ deg from normal and is focused onto a target which is parallel to the lens. This oblique focusing geometry has several advantages over the normal incidence arrangements used in previous work.^{1,8} The large angle of incidence expands the length of the line focus by $1/\cos\theta$; therefore, our 3.3 cm diameter beam produces a 9 cm long plasma. In addition, the pump laser sweeps across the target, and the leading edge of the plasma travels at a speed, $c/\sin\theta$, only 8% greater than that of light. The emitted soft x-rays thus provide nearly synchronous traveling-wave excitation of the ambient gaseous medium.

In order to reduce the pump energy lost to grazing incidence reflection, grooves were cut into the target surface at a 45 deg angle, as shown in the inset of Fig. 2. The grooved surface decreases the local angle of incidence of the p-polarized pump laser from 68 deg to 23 deg and divides the input beam to form many small, separated plasmas rather than one continuous line. The combined length of these plasmas is only slightly greater than the input beam diameter. As a result, the extended gain length can be pumped with increased 1064 nm intensity and improved soft x-ray conversion efficiency.

All of the experiments described here were performed with a 3.5 J, 300 psec FWHM pump laser with a repetition rate of 1 shot every 5 minutes. The 3.3 cm diameter, spatially uniform, input beam was compressed (using normal incidence cylindrical optics) to 1.7 cm in the focusing dimension to increase the f -number of the lens and reduce aberrations. The focal length of the oblique cylindrical lens can be approximated by the sagittal focal length of a tilted spherical lens; for $f_0 = 20$ cm and $\theta = 68$ deg, the focal length is 12 cm. A 2.5 cm diameter stainless steel rod, threaded at 19 grooves cm^{-1} and electroplated with gold, served as the target. This arrangement produced a focal line width of 200 μm and an intensity on target of about $2 \times 10^{11} \text{ W cm}^{-2}$. The ambient Xe pressure was 4 torr.



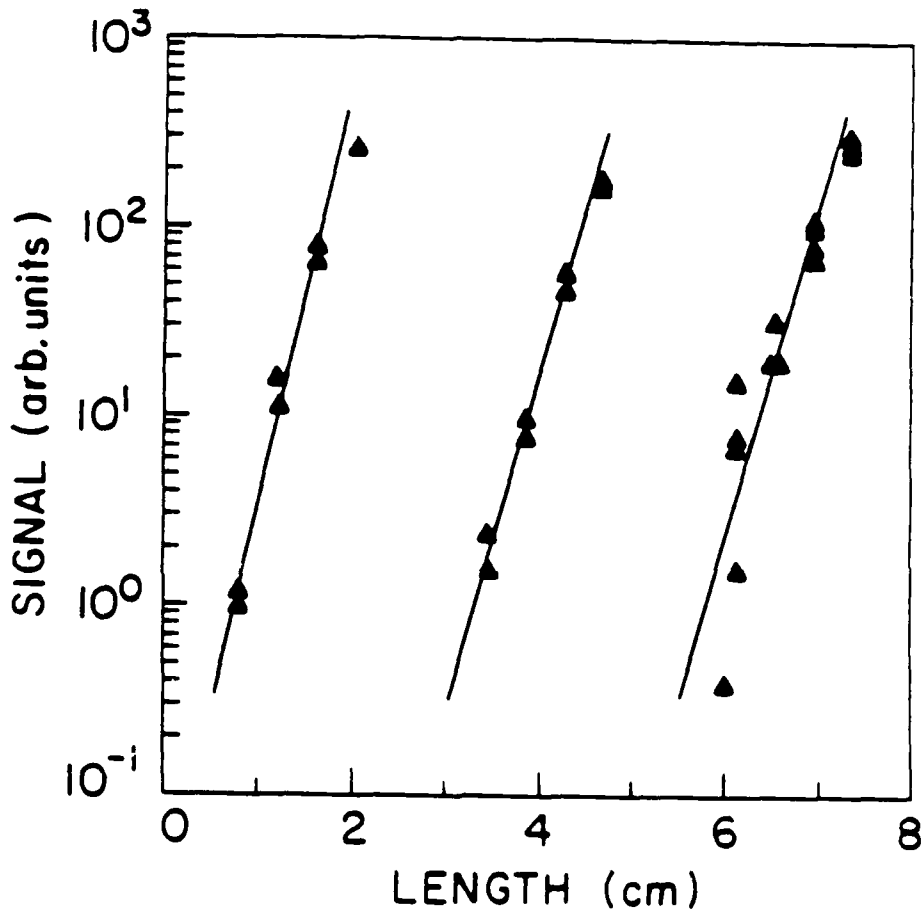
5765-3

Fig. 2 Traveling-wave laser-produced-plasma soft x-ray source.

The observed excited volume was defined by two plates separated by 1.5 mm, through which the 1064 nm pump laser was focused, and by two 2 mm diameter pinholes on an axis 1.5 mm above the target and located 2 cm from the ends of the line focus. We monitored the 109 nm emission in the forward and backward directions simultaneously using two 0.2 m VUV monochrometers coupled to windowless channel electron multipliers. A 1 mm thick LiF window isolated each of the monochrometers from the Xe cell. To avoid saturation of the electron multipliers, we used calibrated LiF and O₂ gas cell attenuators to achieve the 10⁵ dynamic range required in these experiments.

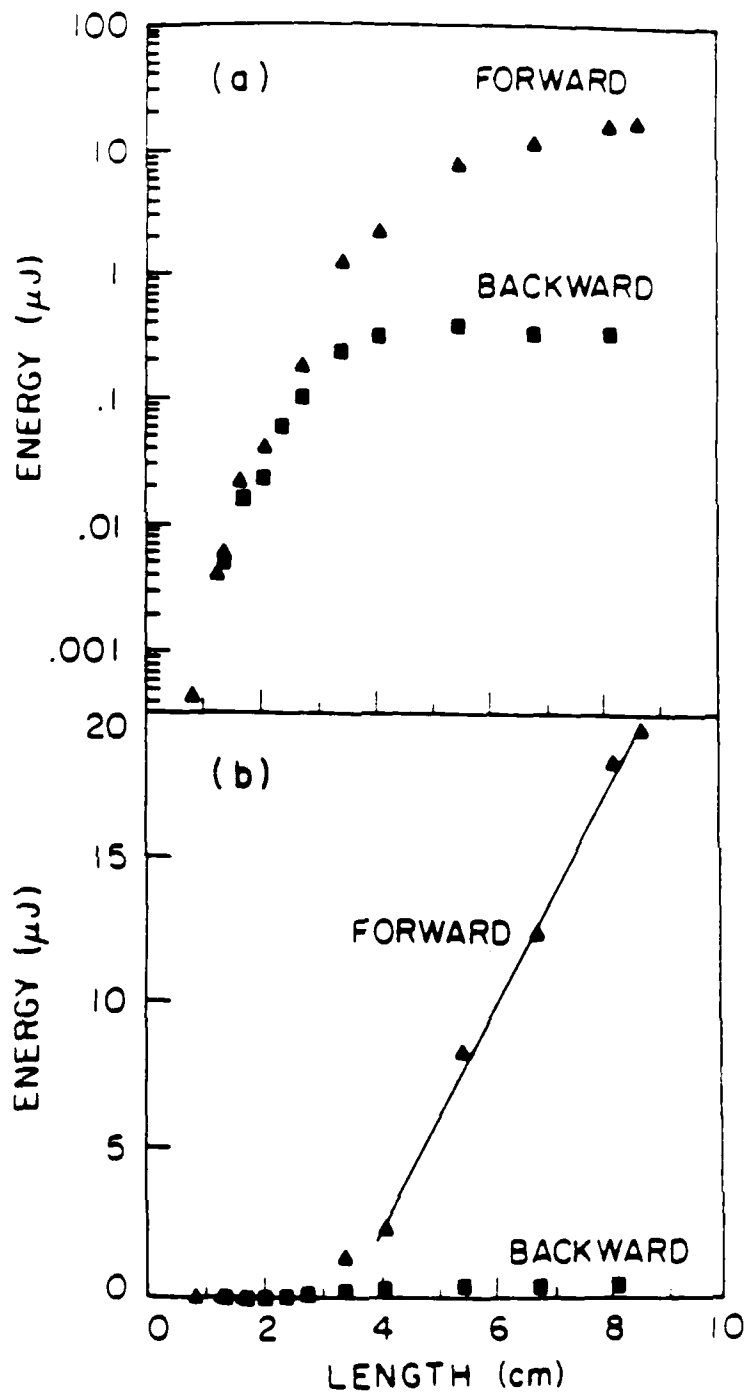
The small-signal gain on the 109 nm transition was determined from measurements of time-integrated emission (the 109 nm pulses were shorter than the 700 psec response time of the detection system) as a function of length. The length of plasma on the target, and hence of the gain medium, was varied by masking the input laser beam. Figure 3 shows the increase in forward-propagating emission with length for three short sections of the target. A simple exponential fit to the data yields an average, time-integrated, small-signal gain coefficient of 4.4 cm⁻¹. This is a 70% improvement over the value obtained with a smooth, gold-plated target. Based on the measured, uniform small-signal gain coefficient, unsaturated amplification along the full 9 cm of length would provide a total gain of exp(40), or 170 dB.

The large-signal behavior of both the forward and backward 109 nm laser emission is shown in the semi-log and linear plots of Figs. 4a and 4b, where each symbol represents the average of at least three data points. For short gain lengths, the slopes of the forward and backward energy vs. length curves (on the log scale in Fig. 4a) are approximately the same. Beyond 4 cm of length, the forward beam grows linearly (Fig. 4b) while the backward emission remains constant. This behavior indicates that the forward beam is fully saturated and is extracting nearly all the stored energy from the second half of the length.



5765-4

Fig. 3-109 nm signal versus length for three different sections of the target. The average exponential gain coefficient is 4.4 cm^{-1} .



5765-8

Fig. 4-109 nm energy versus plasma length on (a) log scale, (b) linear scale showing saturated, linear growth of the forward beam.

The vertical scale of Fig. 4 was calibrated in units of energy by replacing the monochrometer-based detection systems with a fast (350 psec), NBS-calibrated vacuum photodiode (Al_2O_3 photocathode) and calibrated LiF window. The increase of energy with length was identical to that in the emission measurements made using the monochrometers. The maximum energy output was $20 \mu\text{J}$ in the forward direction and $0.4 \mu\text{J}$ in the backward direction, yielding a forward-to-backward emission ratio of 50 : 1.

By visual observation of fluorescence on a scintillator located 90 cm from the target, and by translation of the vacuum photodiode in this plane, we estimate a forward beam divergence of 10 mrad. This small divergence is consistent with the large aspect ratio (length / width ≈ 60) of the geometry. The pulsewidth of the 109 nm laser emission was less than the 350 psec time resolution of the photodiode, which implies an output power greater than 50 kW.

Assuming the measured energy is extracted predominantly from the last 6 cm of gain length, the total energy stored in the observed volume is $30 \mu\text{J}$, or about 10^{-5} of the 1064 nm pump energy. Taking the cross sectional area of the laser to be 0.03 cm^2 , we calculate an energy density of $110 \mu\text{J cm}^{-3}$ stored in the 109 nm inversion. Given the atomic parameters of the system,² i.e. an average 4d photoionization cross section of 15 Mb between 70 and 130 eV, the 5% Auger yield, and $\sim 12\%$ quantum efficiency, we can deduce a conversion efficiency of 1064 nm light to useful soft x-rays of approximately 2%.

The relationship of the observed gain behavior to the measured stored energy is complicated by the transient nature of the population inversion. The spontaneous lifetime of the upper level is 4.75 nsec,² but the inversion lifetime and pulse length are governed by stimulated decay and are on scale with the transit time of the gain medium. The large forward-to-backward emission ratio imparted by the traveling-wave excitation can be explained in terms of competition between the two beams. Although the slopes of the forward and backward energy vs. length curves in Fig. 4a are similar for the shorter lengths,

the forward beam reaches saturation earlier and, therefore, dominates in the second half of the length.

In this work we have demonstrated single-pass gain saturation of a photoionization-pumped laser. We have employed a traveling-wave laser-produced-plasma geometry which efficiently excites an extended gain length using only a few joules of pump energy. These results represent a significant step in the development of practical photoionization-pumped lasers.

The authors would like to thank G. Y. Yin for helpful discussions, and H. N. Kornblum of Lawrence Livermore National Laboratories for the use of the vacuum photodiode. M. H. Sher gratefully acknowledges the support of an AT&T Ph.D. Scholarship. J. J. Macklin gratefully acknowledges the support of an IBM Fellowship. This work was jointly supported by the U.S. Office of Naval Research, the U.S. Air Force Office of Scientific Research, the U.S. Army Research Office, the Strategic Defense Initiative Organization, and Lawrence Livermore National Laboratories.

References

1. H. C. Kapteyn, R. W. Lee, and R. W. Falcone, "Observation of a short-wavelength laser pumped by Auger decay," *Phys. Rev. Lett.* **57**, 2939-42 (1986).
2. H. C. Kapteyn, M. M. Murnane, R. W. Falcone, G. Kolbe, and R. W. Lee, "Measurements on a proposed short wavelength laser system in xenon III," *Proc. Soc. Photo-Opt. Instrum. Eng.* **688**, 54 (1986).
3. M. A. Duguay, "Soft x-ray lasers pumped by photoionization," in *Laser Induced Fusion and X-Ray Laser Studies*, S. F. Jacobs, M. O. Scully, M. Sargent III, and C. D. Cantrell III, eds. (Addison-Wesley, Reading, Mass., 1976), p. 557.
4. E. J. McGuire, "Soft-x-ray amplified spontaneous emission via the Auger effect," *Phys. Rev. Lett.* **35**, 844-848 (1975).
5. R. G. Caro, J. C. Wang, R. W. Falcone, J. F. Young, and S. E. Harris, "Soft x-ray pumping of metastable levels of Li^+ ," *Appl. Phys. Lett.* **42**, 9-11 (1983).
6. W. T. Silfvast, J. J. Macklin, and O. R. Wood II, "High-gain inner-shell photoionization laser in Cd vapor pumped by soft-x-ray radiation from a laser-produced plasma source," *Opt. Lett.* **8**, 551-3 (1983).
7. A. J. Mendelsohn and S. E. Harris, "Proposal for an extreme-ultraviolet selective autoionization laser in Zn III," *Opt. Lett.* **10**, 128-130 (1985).
8. Guang-Yu Yin, C. P. J. Barty, D. A. King, D. J. Walker, S. E. Harris, and J. F. Young, "Low-energy pumping of a 108.9-nm xenon Auger laser," *Opt. Lett.* **12**, 331-3 (1987).

Figure Captions

1. Energy level diagram of Xe showing the levels relevant to photoionization and to Auger pumping of Xe III.
2. Traveling-wave laser-produced-plasma soft x-ray source.
3. 109 nm signal versus length for three different sections of the target. The average exponential gain coefficient is 4.4 cm^{-1} .
4. 109 nm energy versus plasma length on (a) log scale, (b) linear scale showing saturated, linear growth of the forward beam.

Section 4

Observation of Super Coster-Kronig Pumped Gain in ZnIII

Observation of Super Coster-Kronig Pumped Gain in Zn III*

D. J. Walker, C. P. J. Barty, G. Y. Yin, J. F. Young, and S. E. Harris

Edward L. Ginzton Laboratory

Stanford University

Stanford, CA 94305

Abstract

We report the observation of laser gain in the vacuum ultraviolet pumped by super Coster-Kronig decay. Using a 5 J, 300 psec pump pulse of 1064 nm radiation, we have observed gain on transitions in Zn III at 127.0 nm, 130.6 nm, and 131.8 nm with total gains of $\exp(2.4)$, $\exp(5.1)$, and $\exp(3.2)$, respectively. The large branching ratios of the rapid super Coster-Kronig decay into a small number of final levels makes high efficiency operation possible.

* This work was jointly supported by the U.S. Air Force Office of Scientific Research, the U.S. Army Research Office, the U.S. Office of Naval Research, Lawrence Livermore National Laboratory, and the Strategic Defense Initiative Organization.

Observation of Super Coster-Kronig Pumped Gain in Zn III

D. J. Walker, C. P. J. Barty, G. Y. Yin, J. F. Young, and S. E. Harris

Edward L. Ginzton Laboratory

Stanford University

Stanford, CA 94305

The use of selective Auger decay to produce population inversion and gain in the soft x-ray and ultraviolet spectral regions was proposed by McGuire¹ in 1975. The first successful experiments were performed by Kapteyn *et al.*² in 1986; in those experiments 55 J of 1064 nm pump energy was used to produce incoherent soft x-rays which photoionized Xe I. These atoms Auger decayed to Xe III to produce a gain of $\exp(7)$ at 109 nm. Experiments by Yin *et al.*³ showed that comparable gains on this transition could be obtained with less than 1 J of pumping energy. Very recently, Sher *et al.*⁴ have used a traveling wave geometry to obtain a small signal gain of $\exp(40)$ and a saturated output energy of $20 \mu\text{J}$ at 109 nm.

In this Letter we follow the proposal of Mendelsohn and Harris⁵ to obtain gain by selective super Coster-Kronig decay of photoionization pumped Zn I. A super Coster-Kronig decay process is a sub-class of an Auger process in which the initial hole, the jumping electron, and the departing electron all occupy the same n shell. As a result, the decay rate is very fast (typically $> 10^{15} \text{ sec}^{-1}$) and therefore, the process dominates other Auger processes. In particular, the branching ratio to the upper level for the Zn system described here is 27% while that to the lower laser level is $< 1\%$. For the 109 nm Xe system, the Auger decay rates to the upper and lower laser levels are about equal,⁶ and an inversion results from the higher degeneracy of the lower level.

We have observed gain on transitions in Zn III at 127.0 nm, 130.6 nm, and 131.8 nm with total gains of $\exp(2.4)$, $\exp(5.1)$, and $\exp(3.2)$, respectively.

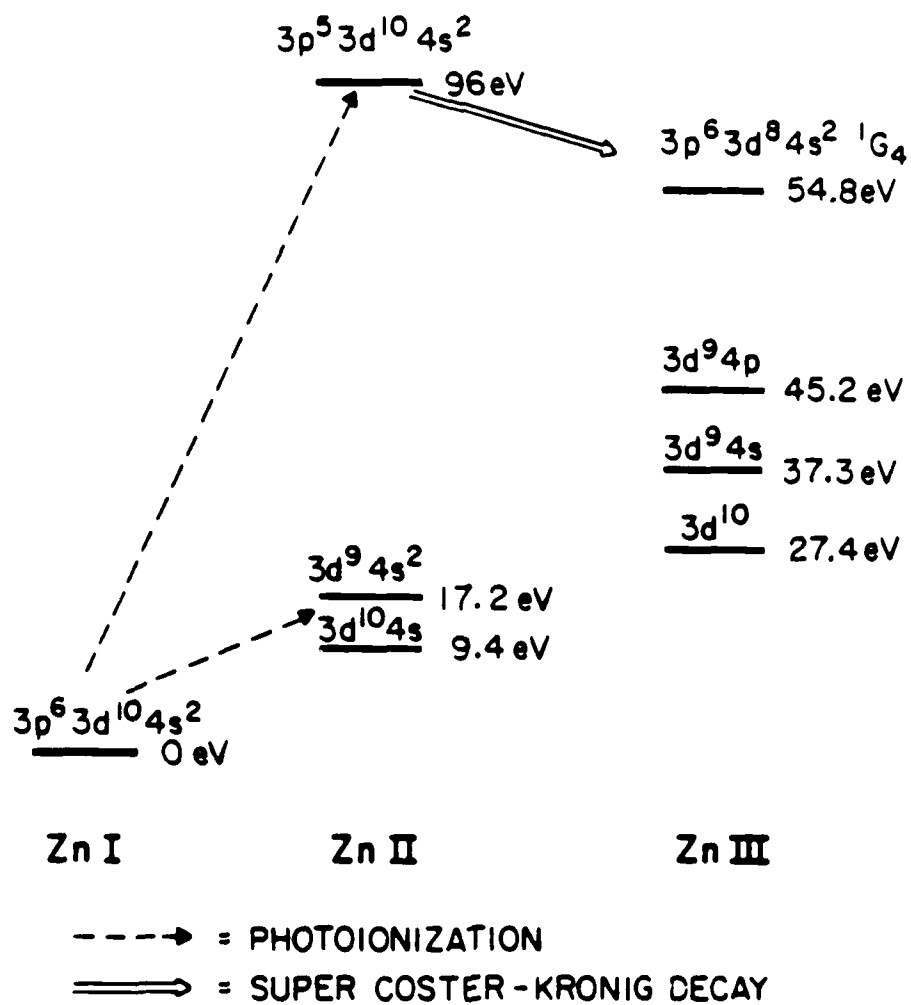


Fig. 1—Simplified energy level diagram of Zn I, Zn II, and Zn III. The branching ratio into the Zn III $3d^8 4s^2 \ ^1G_4$ level is 27%.

The relevant energy levels of the Zn system are shown in Fig. 1. Photoionization of Zn I $3p^63d^{10}4s^2$ ground level atoms by the x-rays emitted by a laser-produced plasma results in the production of highly excited Zn II $3p^53d^{10}4s^2$ ions. These ions undergo rapid, selective, MMM super Coster-Kronig decay into levels of Zn III. Calculations^{5,7} have shown that about 48% of this decay produces the Zn III $3p^63d^84s^2$ 4G_4 L-S basis level. Configuration mixing of the Zn III $3d^84s^2$ configuration with the nearby Zn III $3d^94d$ configuration results in several levels of both configurations having significant components of the $3d^84s^2$ 4G_4 basis level. Thus, they receive a large fraction of the super Coster-Kronig decay. The energy levels relevant to the transitions on which we have observed gain, and the branching ratios into them, are shown in Fig. 2. The level positions are from Dick,⁸ and the branching ratios and gain cross-sections are from Refs. 5 and 7.

Our experimental configuration, shown in Fig. 3, is similar to that suggested by Harris *et al.*⁹ and demonstrated by Caro *et al.*,¹⁰ Silfvast *et al.*,¹¹ and Lundberg *et al.*¹² The 5 J, 300 psec, 1064 nm pump laser is focused by a 30 cm focal length cylindrical lens, producing a focal line 28 mm long by $\sim 100 \mu\text{m}$ wide. The beam passes through a 1.5×28 mm long slotted aperture positioned 2 mm from, and parallel to, the solid Ta target in the Zn cell. This slot defines both the pumped volume and the volume observed by the detection system. The detection system consists of a 1 m normal-incidence vacuum monochromator followed by a p-terphenyl scintillator and a fast visible photomultiplier tube. The system has a total response time of about 5 ns FWHM. The Zn cell is a heat pipe oven with He buffer gas operating at about 500 C. Because the operating temperature is so close to the melting point of Zn, 418 C, the heat pipe wicks are not very effective in returning condensed Zn to the hot zone, and the cell has a tendency to deplete after about 1 hr of operation. The Zn cell is separated from the spectrometer by a LiF window.

The gains of the Zn transitions were measured by blocking parts of the pump beam to vary the length of the pumping plasma and measuring the resulting output energy. The actual output beam of our laser is 32 mm in diameter, but 2 mm of each edge of the beam

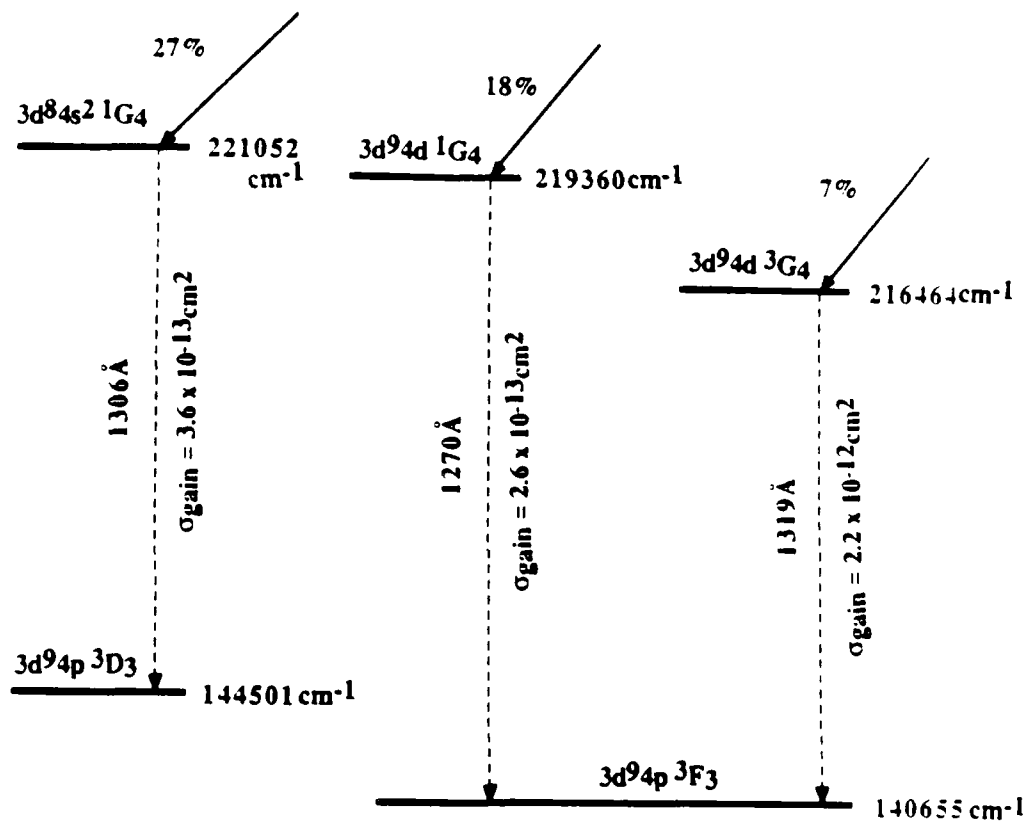


Fig. 2—Energy level diagram of the transitions on which gain was observed.

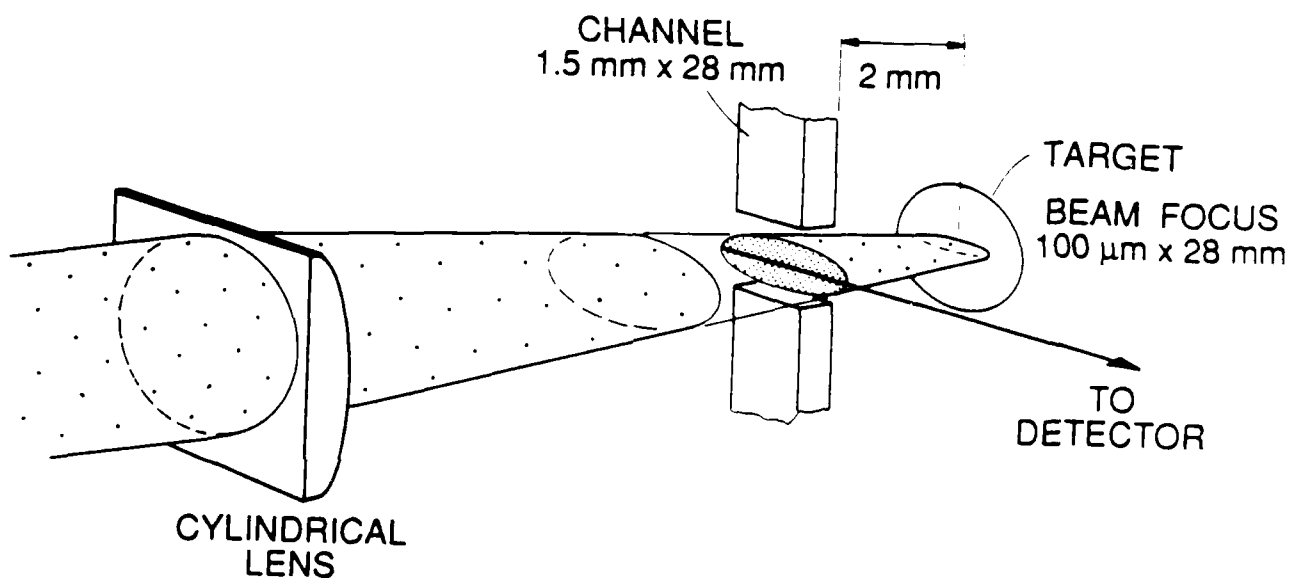


Fig. 3—Schematic of experimental configuration.

was permanently blocked to equalize the energy per unit area of different vertical strips of the beam. The measured energy as a function plasma length was fit to the theoretical frequency-integrated emission function of a line radiator, which can be approximated as¹³

$$E \propto \frac{[\exp(\alpha l) - 1]^{3/2}}{[\alpha l \exp(\alpha l)]^{1/2}} \quad (1)$$

where α is the gain per unit length and l is the length. The points on Fig. 4 are measured values of 130.6 nm energy and the curve is the best fit of Eq. 1 to those points. In this case the fit indicates $\alpha = 1.7 \text{ cm}^{-1}$ and a total gain of $\exp(4.8)$. This method was used to determine all of the gain values presented here. We estimate our minimum measurable gain to be about 0.7 cm^{-1} . The measured values varied about 20% from day-to-day, largely because of variations in the performance of the Zn cell.

Figure 5 shows that the gain at 130.6 nm maximizes at a Zn pressure of about 1.2 torr. The decrease in gain at higher pressure is probably due to electron quenching of the upper level population. In Zn I, the largest photoionization cross section is for the removal of a 3d electron, not a 3p electron.¹⁴ Thus, a large number of electrons are produced that are not involved in creating excited states, but which can act to destroy the inversion by processes such as electron de-excitation or ionization of the upper level.

In addition to measuring the gain at 127.0 nm, 130.6 nm, and 131.8 nm, we also looked for gain at 130.3 nm, 133.2 nm, 135.9 nm, and 136.3 nm, using the 1.2 torr optimum pressure. These transitions have upper levels that are populated by super Coster-Kronig decay and could conceivably have gain. We did not observe gain above our minimum threshold at any of these wavelengths. We note that the 133.2 nm transition, which shares an upper level with the 130.6 nm transition, was predicted⁵ to have the higher gain; we did not observe this to be the case.

In summary, using only several joules of laser energy, we have observed super Coster-Kronig pumped gain on several transitions near 130 nm. As shorter wavelength systems and deeper holes are accessed, the high selectivity and ease of identification of the super

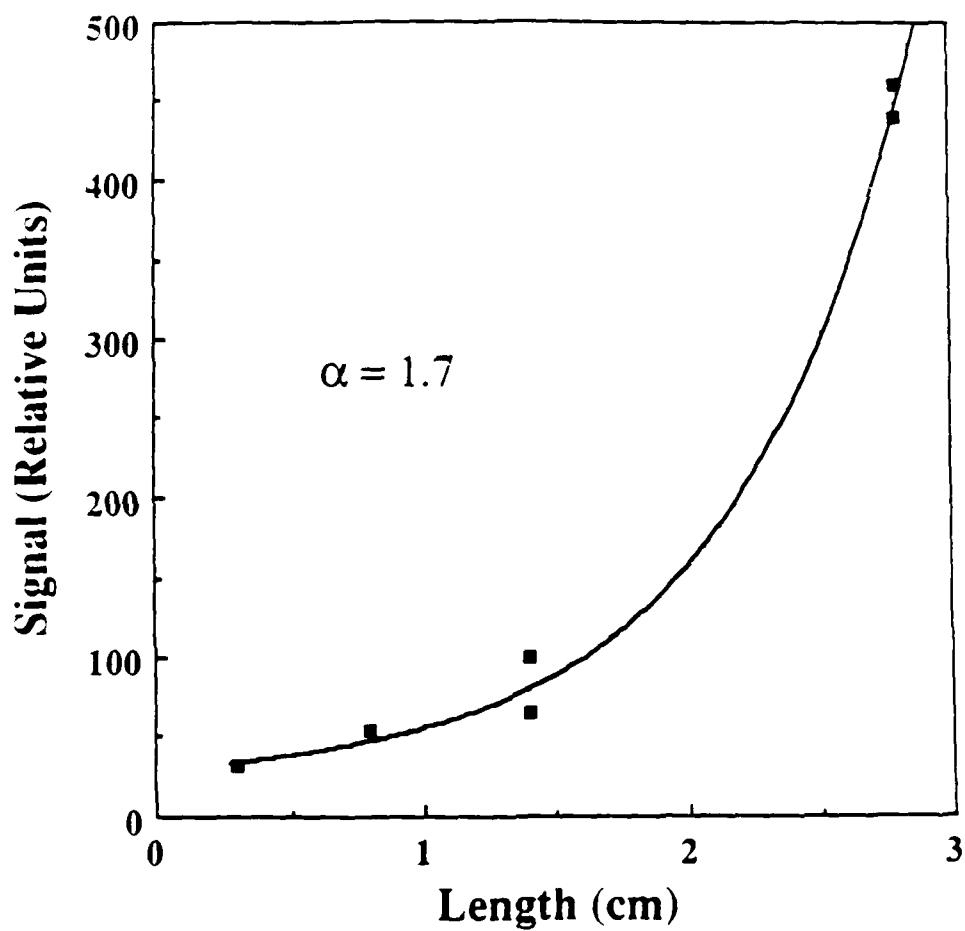


Fig. 4—Output energy at 130.6 nm as a function of pumped length for a plasma-producing laser energy of 5 J in a 300 psec pulse and Zn pressure of 1.2 torr.

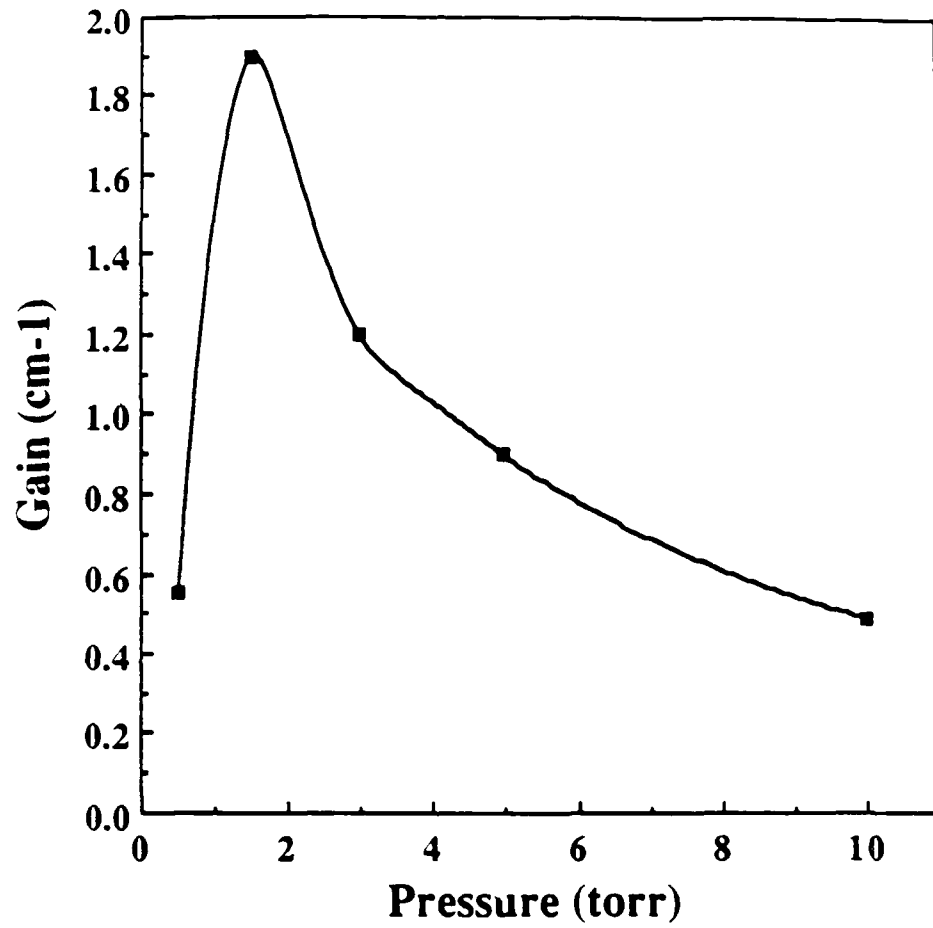


Fig. 5—Gain coefficient as a function of Zn pressure at 130.6 nm for a 5 J, 300 psec long pump pulse.

Coster-Kronig process will make it important not only for directly pumped systems, but also for systems which are pumped by Auger cascade.

The authors thank A. J. Mendelsohn for helpful discussions. This work was jointly supported by the U.S. Air Force Office of Scientific Research, the U.S. Army Research Office, U.S. Office of Naval Research, Lawrence Livermore National Laboratory, and the Strategic Defense Initiative Organization.

References

1. E. J. McGuire, "Soft x-ray amplified spontaneous emission via the Auger effect," *Phys. Rev. Lett.* **35**, 844-848 (1975).
2. H. C. Kapteyn, R. W. Lee, and R. W. Falcone, "Observation of a short-wavelength laser pumped by Auger decay," *Phys. Rev. Lett.* **57**, 2939-42 (1986).
3. Guang-Yu Yin, C. P. J. Barty, D. A. King, D. J. Walker, S. E. Harris, and J. F. Young, "Low-energy pumping of a 108.9 nm xenon Auger laser," *Opt. Lett.* **12**, 331-3 (1987).
4. M. H. Sher, J. J. Macklin, J. F. Young, and S. E. Harris, "Saturation of the Xe III 109 nm laser using a traveling wave laser-produced plasma" (unpublished).
5. A. J. Mendelsohn and S. E. Harris, "Proposal for an extreme-ultraviolet selective autoionization laser in Zn III," *Opt. Lett.* **10**, 128-130 (1985).
6. H. C. Kapteyn, M. M. Murnane, R. W. Falcone, G. Kolbe, and R. W. Lee, "Measurements on a proposed short wavelength laser system in Xe III," *Proc. Soc. Photo-Opt. Instrum. Eng.* **688**, 54-60 (1986).
7. A. J. Mendelsohn, "Extreme ultraviolet emission spectroscopy of atoms and laser applications," Ph. D. dissertation (Stanford University, Stanford, California, 1985).
8. K. A. Dick, "The spark spectra of zinc. II. zinc III," *Can. J. Phys.* **46**, 1291-1302 (1968).

9. S. E. Harris, J. F. Young, R. W. Falcone, Joshua E. Rothenberg, J. R. Willison, and J. C. Wang, "Anti-stokes scattering as an XUV radiation source and flashlamp," in *Laser Techniques for Extreme Ultraviolet Spectroscopy*, T. J. McIlrath and R. R. Freeman, eds. (New York: AIP, 1982), pp. 137-152.
10. R. G. Caro, J. C. Wang, R. W. Falcone, J. F. Young, and S. E. Harris, "Soft x-ray pumping of metastable levels of Li^+ ," *Appl. Phys. Lett.* **42**, 9-11 (January 1983).
11. W. T. Silfvast, J. J. Macklin, and O. R. Wood II, "High-gain inner-shell photoionization laser in Cd vapor pumped by soft x-ray radiation from a laser-produced plasma source," *Opt. Lett.* **8**, 551-3 (1983).
12. H. Lundberg, J. J. Macklin, W. T. Silfvast, and O. R. Wood II, "High-gain soft-x-ray-pumped photoionization laser in zinc vapor," *App. Phys. Lett.* **45**, 335-7 (1984).
13. G. J. Linford, E. R. Peressini, W. R. Sooy, and M. L. Spaeth, "Very long lasers," *App. Optics* **13**, 379-390 (1974).
14. A. W. Fliflet and H. P. Kelley, "Photoionization of the $3d$, $3p$, and $3s$ subshells of Zn I ," *Phys. Rev. A* **13**, 312-317 (1976).

List of Figures

1. Simplified energy level diagram of Zn I, Zn II, and Zn III. The branching ratio into the Zn III $3d^8 4s^2 \ ^1G_4$ level is 27%.
2. Energy level diagram of the transitions on which gain was observed.
3. Schematic of experimental configuration.
4. Output energy at 130.6 nm as a function of pumped length for a plasma-producing laser energy of 5 J in a 300 psec pulse and Zn pressure of 1.2 torr.
5. Gain coefficient as a function of Zn pressure at 130.6 nm for a 5 J, 300 psec long pump pulse.

Section 5

Supported Publications and Presentations

Publications

N00014-86-C-2361

1. Guang-Yu Yin, C. P. J. Barty, D. A. King, D. J. Walker, S. E. Harris, and J. F. Young, "Low Energy Pumping of a 108.9 nm Xe Auger Laser," *Opt. Lett.* **12**, 331-333 (May 1987).
2. M. H. Sher, J. J. Macklin, J. F. Young, and S. E. Harris, "Saturation of the XeIII 109 nm Laser Using Traveling-Wave Laser-Produced-Plasma Excitation" (in preparation).
3. D. J. Walker, C. P. J. Barty, G. Y. Yin, J. F. Young, and S. E. Harris, "Observation of Super Coster-Kronig Pumped Gain in ZnIII" (in preparation).

Presentations

N00014-86-C-2361

1. "Saturation of the Xe III 109 nm Laser using Traveling-Wave Laser-Produced-Plasma Excitation," *XV International Conference on Quantum Electronics, (IQEC '87)*, Baltimore, Maryland, April 1987 (post deadline).
2. "Optimization of Gain at 108.9 nm in Xe III," *XV International Conference on Quantum Electronics, (IQEC '87)*, Baltimore, Maryland, May 1987.
3. "Short Wavelength Lasers Based on Selective Auger Processes and Core-Excited Metastable Levels," *SDIO*, Huntsville, Alabama, May 1987.

END

DATE

FILMED

4-88

DTIC